JMEPEG (2012) 21:1447–1454
DOI: 10.1007/s11665-011-0021-2

1059-9495/$19.00

Influence of Nickel and Manganese on Microstructure and Mechanical Properties of Shielded Metal Arc-Welded API-X80 Steel

Fariba Sheykh Jaberi and A.H. Kokabi

(Submitted December 17, 2010)

Microstructure developments of X80 weld metal by the addition of different amounts of alloying elements such as nickel and manganese to the covering of electrodes were investigated. For this reason, samples were welded with electrodes that Ni value has changed between 0.8 and 3.5% in two critical amounts of Mn 0.7 and 1.6. Optical microscopy and scanning electron microscopy were applied for peer investigation of microstructure. Different phase percentages were obtained by Clemex software and compared in all samples. Results indicated that Ni and Mn change weld microstructure in the as-deposited zone and reheated part and corresponding to each alloying element concentration, amount of acicular ferrite, as a determining factor for mechanical properties, were changed.

Keywords acicular ferrite, alloying elements, API-X80, microstructure, pipe line, welding

1. Introduction

There have been ongoing developments in high-strength steel weld metals with the aim of increasing strength while maintaining acceptable toughness since the 1960s (Ref 1). Mechanical properties of welds are determined by chemical composition, cooling rate (technological parameters such as voltage and current) and microstructure, in fact microstructure is a function of the other variables (Ref 2). To achieve optimal combination of strength and toughness, new grades of low alloy steels such as API-5L X80 for offshore constructions and line piping have been designed and developed (Ref 2, 3). Research has been carried out based on fundamental understanding of the effects of alloying on phase transformations and microstructure to develop new improved compositions. Ultimately, the aim has been to achieve weld metal properties that surpass established commercial weld metals and show less sensitivity to welding parameters (Ref 1). Alloying additions in the majority of weld metals are usually kept to a minimum to avoid the formation of brittle phases and defects, such as cold cracks inside the weld. This is related to the hardenability of the weld metal, which has to be low enough in order to avoid the transformation of residual austenite to relatively high carbon martensite (Ref 4). In the majority of high-strength steel weld metals studied previously, different amounts of microalloying elements (Ref 2-5) or important factors which involved in HAZ properties such as cooling rate (Ref 6) and welding speed (Ref 7) have been investigated. Hence, there were little focuses on effects of main alloying elements on weld metal properties of API-X80. And there is no general agreement regarding the amount and combination proportion ratios of Ni and Mn in weld metal. It has been reported that the weld metal toughness can be increased noticeably by an increase of Ni content (Ref 8). However, some investigations have shown that the benefit from Ni is conditional (Ref 9-11). This study details the effect of Ni and Mn on weld metal properties and metallographic studies were conducted to evaluate the influence of Ni and Mn on hardness, yield strength, tensile strength, and toughness of API-X80 weld metal.

Fariba Sheykh Jaberi and **A.H. Kokabi**, Department of Materials Engineering and Science, Sharif University of Technology (SUT), Tehran, Iran. Contact e-mail: fariba.jaberi1985@gmail.com.

2. Experimental Procedures

2.1 Electrodes

Six experimental, low hydrogen basic electrodes (E8018G base) were designed. The coating ratio of the electrodes was considered as 1.5. Different amounts of alloying powders were added to the coating to produce different levels of manganese and nickel in all weld metal samples, nominally 0.7 and 1.6% Mn and 0.8, 2.4 and 3.2% Ni. Prior to welding, the welding electrodes were baked for 1 h at 350 °C. The chemical composition and codes of different samples have been illustrated in Table 1.

2.2 Weld Preparation

The welding was carried out on API-X80 plate with a nominal chemical composition as shown in Table 2. The thickness of the plate was 19 mm; welding was performed in flat position. The groove filled with 16 layers, each containing three beads, reversing welding direction after each bead. The joint geometry is illustrated in Fig. 1. The interpass temperature and welding parameters are indicated in Table 3.

2.3 Metallographic Study

The transverse section of the weld deposits were prepared from the top beads (Fig. 2) and the adjacent reheated zones and polished by using different grades of emery papers and finally with diamond paste. All metallographic specimens were etched with Nital 2% and examined by light optical microscopy. Further investigations of the microstructure were undertaken by scanning electron microscope (SEM). A Clemex Image Analysis System (professional version 2002) was used for the microstructural observation, grain size evaluation, and quantitative phase analysis.

Table 1 Chemical compositions of experimental specimens weld metals

	Concentration of elements%								
Weld ID	**C**	**Mo**	**Cu**	**Ni**	**Mn**	**Cr**	**Ti**	**P**	**Si**
LNi1	0.070	0.40	0.11	0.79	0.70	0.012	0.009	0.010	0.45
LNi2	0.057	0.40	0.12	2.40	0.71	0.013	0.008	0.008	0.42
LNi3	0.050	0.37	0.12	3.20	0.70	0.013	0.009	0.008	0.44
HNi1	0.085	0.40	0.03	0.76	1.55	0.010	0.010	0.019	0.52
HNi2	0.067	0.41	0.08	2.40	1.60	0.009	0.010	0.008	0.51
HNi3	0.077	0.41	0.02	3.40	1.60	0.006	0.009	0.017	0.53

3. Results and Discussion

3.1 Metallographic Examination

3.1.1 As-Deposited Zone. Figure 2 shows optical micrographs of the microstructures of all samples based on Mn and Ni variations. White intercellular-dendritic boundaries of welds were revealed by etching in Le Pera's etchant. The increased nickel and manganese contents render the intercellular-dendritic boundaries more resistant to etching, and hence, they appear white in the light micrograph. In Fig. 2, the magnification is not high because of revealing overall microstructure. It is simply obvious that up to 2.4% Ni, columnar grain size in both amounts of Mn has reduced but it has extremely increased in 3.2% Ni. As it was mentioned in Zhang investigation (Ref 10), this phenomenon was named as ''elephant structure'' that it is illustrating very wide grains.

For studding the effect of Ni and Mn on amount of different phases, optical micrograph with higher magnification were prepared. The microstructures have been shown in Fig. 3. One of the most important phases in low carbon weld metal is acicular ferrite (AF) and other kinds of ferrite such as side plate ferrite (FS), grain boundary ferrite and secondary phases exist in as-deposited weld metals too. Secondary phases in this zone are composed of pearlite, bainite, carbides, and M-A. The percentages of the various ferrite morphologies including AF

Table 2 Chemical composition of X80 steel

Element	**C**	**Si**	**Mn**	**P**	**S**	**Ni**	**Cr**	**Cu**	**Mo**	**V**	**Nb**	**Ti**	**Al**	**N**
Wt.%	0.072	0.250	1.805	0.0078	0.001	0.26	0.02	0.009	0.29	0.003	0.035	0.012	0.031	0.004

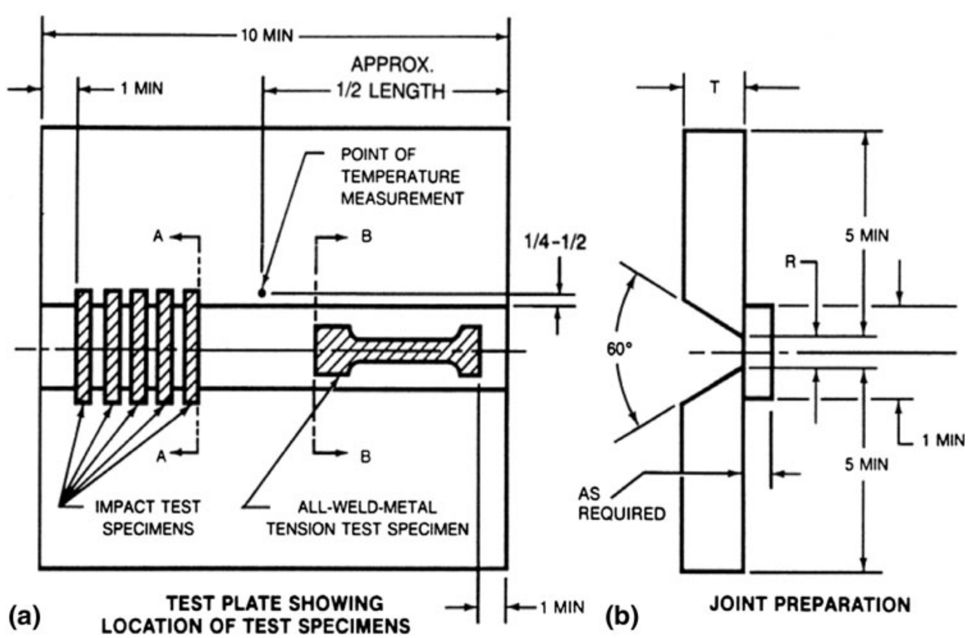

Fig. 1 Schematic diagram of (a) location of test specimen and (b) joint preparation (Ref 12)

and FS are shown in Table 3 and graphically in Fig. 4 for the six welds.

Generally in both groups (L and H), it is obvious that by increasing Ni, microstructure size will decrease and become finer. In L group, Ni effect has been reflected by increasing AF and FS, in expense of decreasing grain boundary ferrite percentage. However, in group H, Ni extremely increases AF, and decreases side plate and grain boundary ferrite at the same time. Finally in 3.2% nickel, side plate percentage reach approximately zero. Noticeable increasing of secondary phases by Ni is in consistent with previous investigations. The reason is that Ni shifts low carbon steel CCT diagram in a manner that some phases such as bainite and martensite forms in the same cooling rates. In addition, Ni is known as a strong austenite stabilizer and increases M-A phase amount too.

In a constant level of Ni, Mn prompted AF and as it was expected the amount of two other kinds of ferrite decrease. Influence of Mn on phase transformation and grain size is similar to Ni, but Mn effect in comparison to Ni, is more noticeable that it can be seen easily from Fig. 3. As an example comparison of LNi3 and HNi3 illustrates that in a constant amount of Ni, the percentage of microphases extremely enhanced by Mn.

Table 3 Columnar grain size and different phase percentages in last pass

Sample ID	Columnar grain size, μm	AF%	PF(G)%	SPF%	Secondary phase%
LNi1	130	42.1	43.7	12.3	1.9
LNi2	53	47.8	28.7	20.2	3.3
LNi3	210	53.8	19.9	21.4	5.2
HNi1	237	62	12.4	1.5	24.1
HNi2	67	77.1	9.2	2.3	11.4
HNi3	250	80.5	1.9	0	17.6

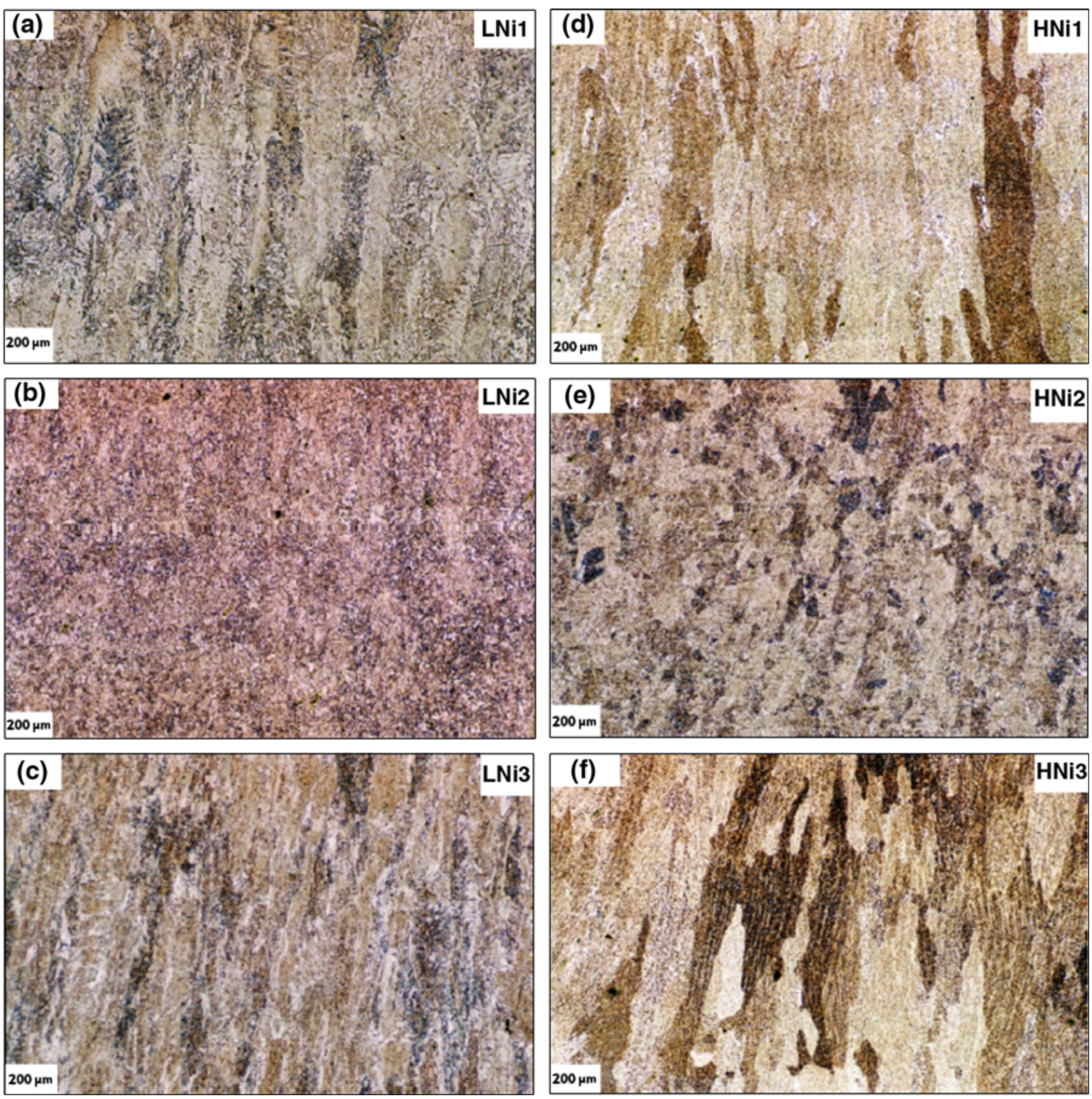

Fig. 2 Optical microstructure of columnar zones of as-deposited weld metals 50×. (a) Mn% = 0.7, Ni% = 0.8, (b) Mn% = 0.7, Ni% = 2.4, (c) Mn% = 0.7, Ni% = 3.2, (d) Mn% = 1.6, Ni% = 1.2, (e) Mn% = 1.6, Ni% = 2.4, and (f) Mn% = 1.6, Ni% = 3.2

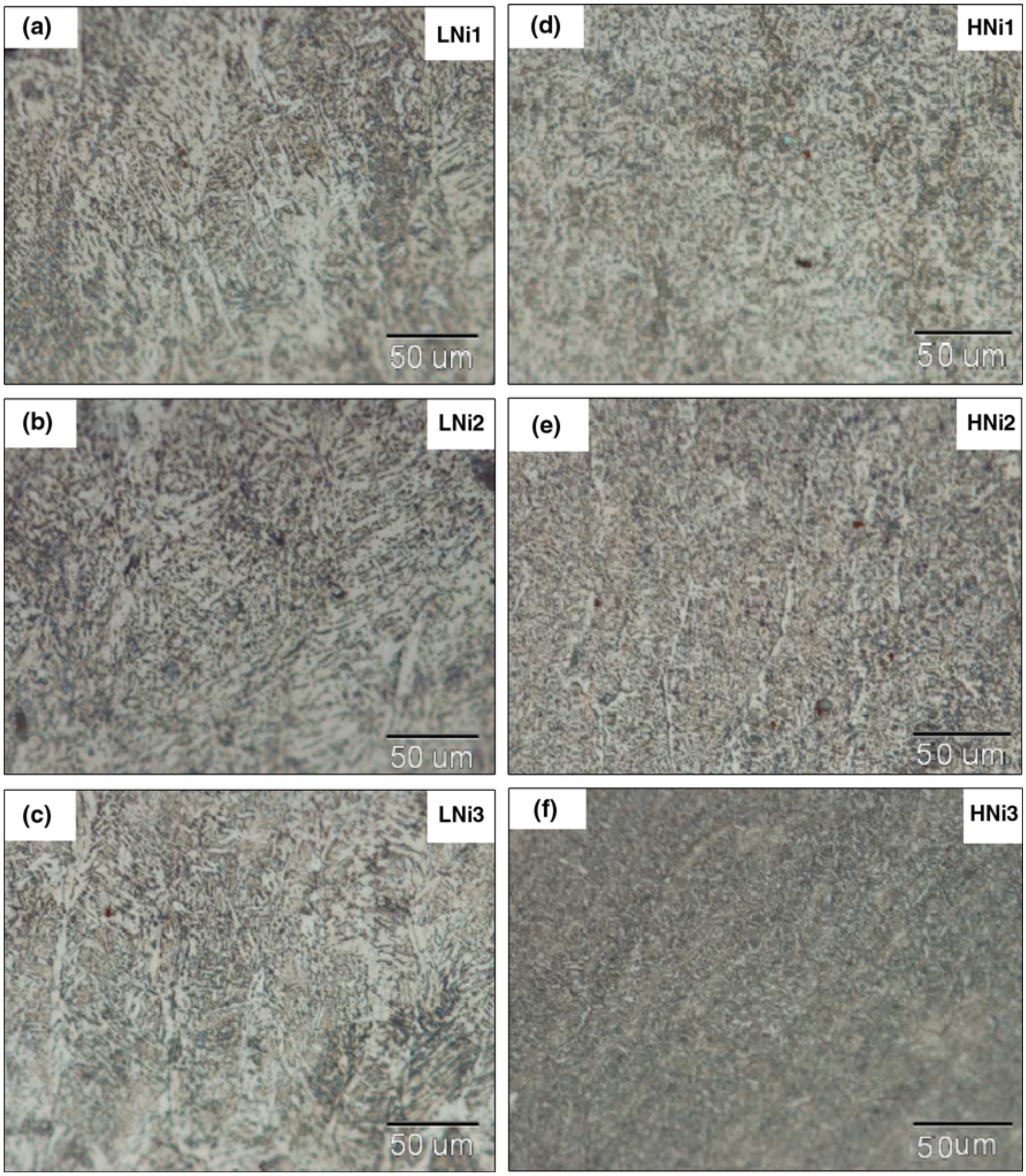

Fig. 3 Optical microstructure of columnar zones of as-deposited weld metals 200×. (a) Mn% = 0.7, Ni% = 0.8, (b) Mn% = 0.7, Ni% = 2.4, (c) Mn% = 0.7, Ni% = 3.2, (d) Mn% = 1.6, Ni% = 1.2, (e) Mn% = 1.6, Ni% = 2.4, and (f) Mn% = 1.6, Ni% = 3.2

3.1.2 Reheated Zone. In multipass welds, more than 50% of weld metals reheat. In this zone, Ni has significant influence on microstructure as it is deducible from Fig. 5. Austenite decomposition during heating and cooling and existence of suitable places for nucleation of ferrite leads to the appearance of different kind of ferrites that amount, size, and distribution of them play an important role in mechanical properties. In this zone, when percentage of alloying elements were low (L group), heat cycle led to a new microstructure in comparison to as-deposited zone. Reheating transformed microstructure to equiaxed or polygonal ferrite. Ni and Mn effectively refined the microstructure of this zone. Figure 6 envelopes SEM results of all samples reheated zone, which demonstrates existence of different phase especially secondary phases and granular bainite. Different phase percentages have been demonstrated in Table 4 and diagrammatically in Fig. 7.

Low manganese samples comparison shows that by increasing Ni microstructure change from polygonal ferrite to AF. In addition, grain sizes reduced significantly. In H group, grain refining is more visible. It means that in high level of Mn, nickel addition is more determining on microstructure. The most important factor for AF nucleation is the non-metallic inclusion.

In this zone similar to as-deposited area, by increasing alloying elements AF increased and primary ferrite decreased.

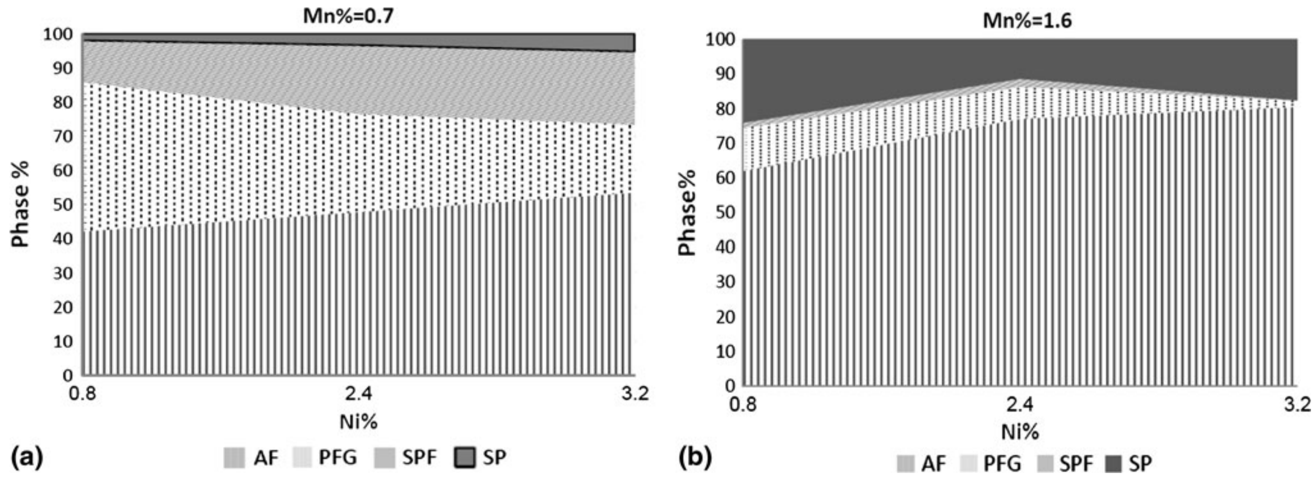

Fig. 4 Different phase amounts in last pass versus Ni and (a) Mn% = 0.7 and (b) Mn% = 1.6

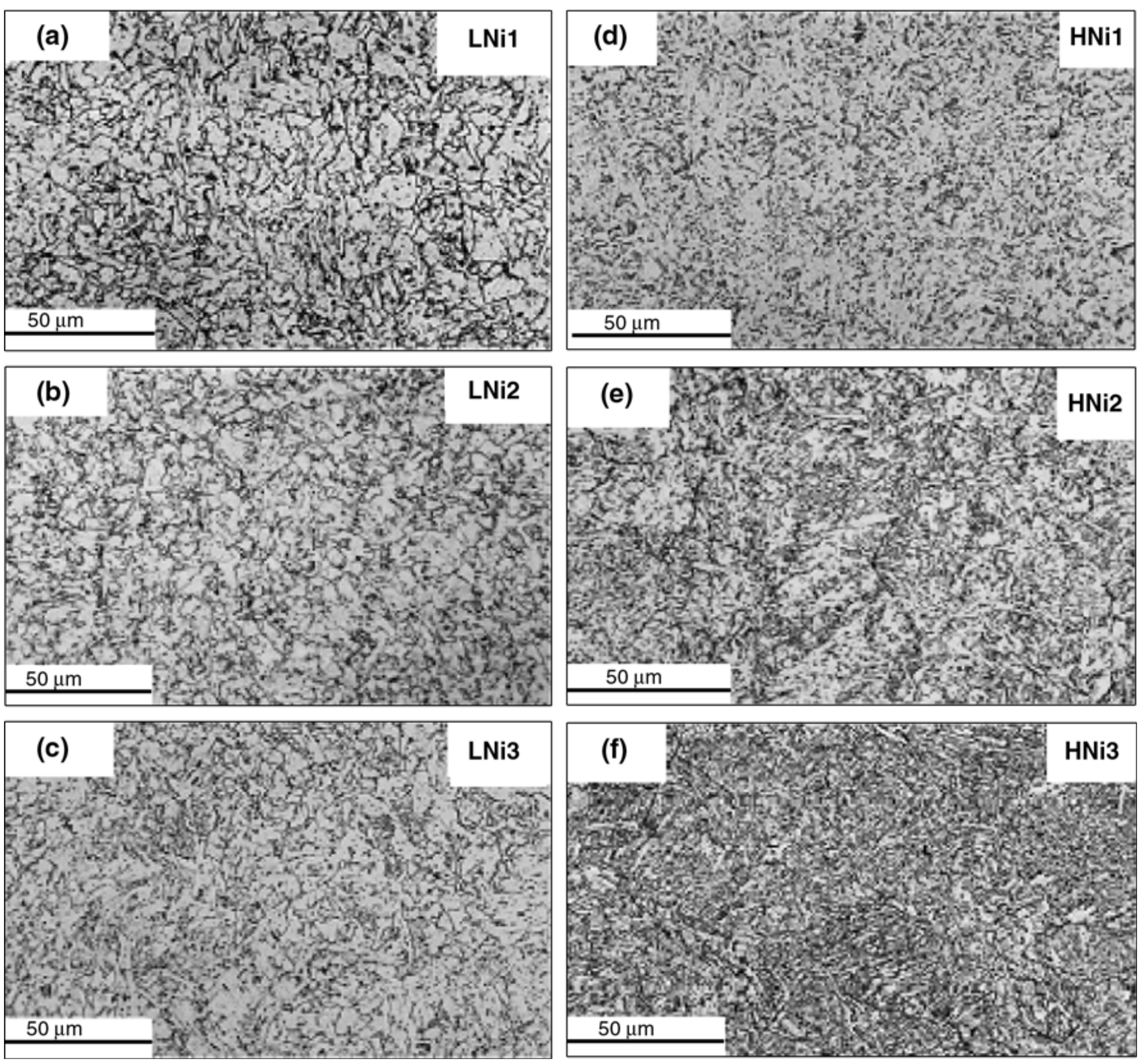

Fig. 5 Reheated zone microstructure 500×. (a) Mn% = 0.7, Ni% = 0.8, (b) Mn% = 0.7, Ni% = 2.4, (c) Mn% = 0.7, Ni% = 3.2, (d) Mn% = 1.6, Ni% = 1.2, (e) Mn% = 1.6, Ni% = 2.4, and (f) Mn% = 1.6, Ni% = 3.2

Very low amount of polygonal ferrite in HNi3 illustrates that microstructure of reheated and as-deposited zone are approximately same in high levels of alloying elements. At high Mn and Ni concentration, grain refining did not occurred in reheated zone. The reason is the reduction of the phase changes according to Ni and Mn addition.

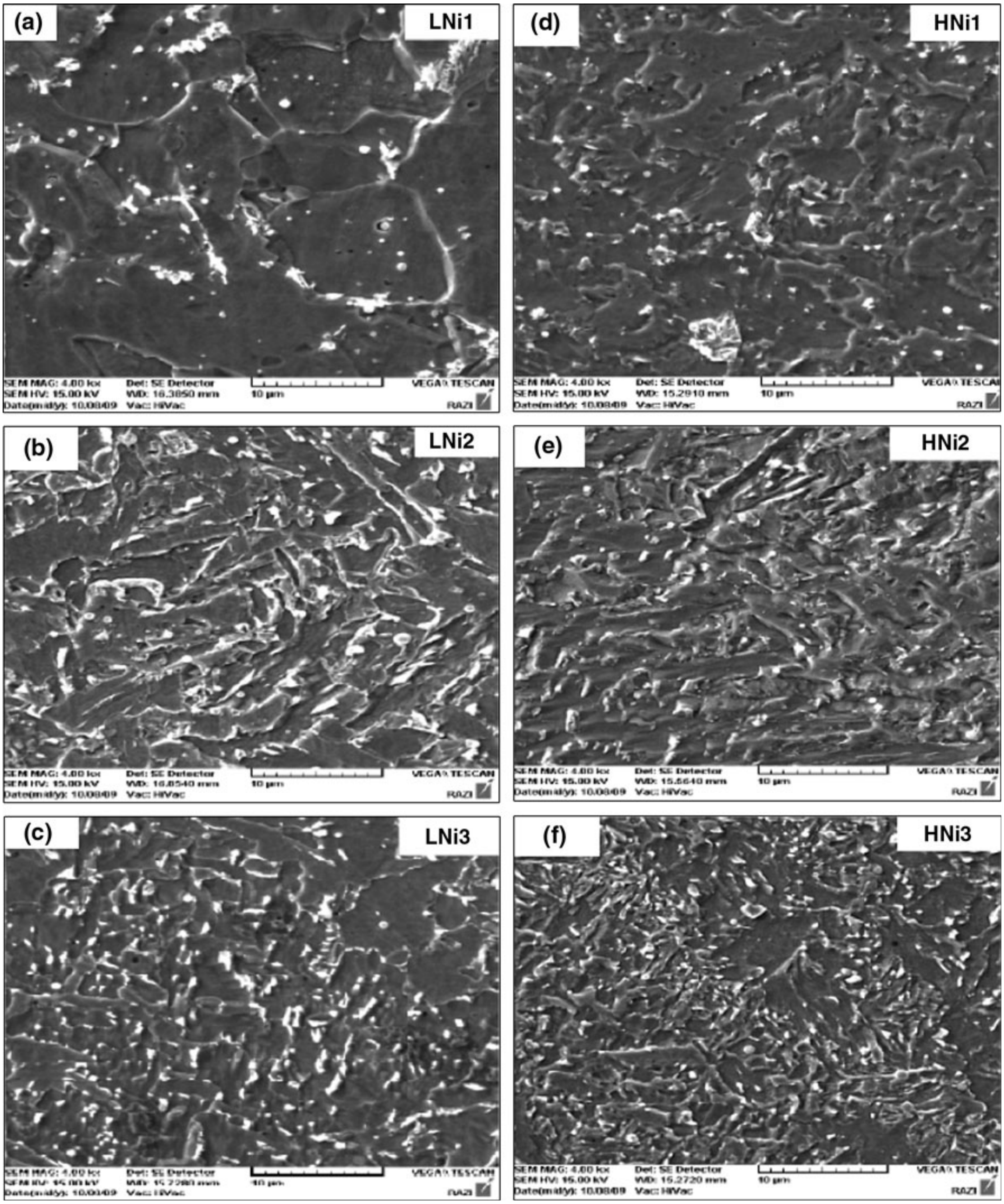

Fig. 6 SEM observing photographs of the reheated zone microstructure 2000×. (a) Mn% = 0.7, Ni% = 0.8, (b) Mn% = 0.7, Ni% = 2.4, (c) Mn% = 0.7, Ni% = 3.2, (d) Mn% = 1.6, Ni% = 1.2, (e) Mn% = 1.6, Ni% = 2.4, and (f) Mn% = 1.6, Ni% = 3.2

Table 4 Different phase percentages of reheated zone

Sample ID	AF%	PF(G)%	GB	Secondary phase%
LNi1	10.6	54.3	33.6	15
LNi2	18	25.5	54.7	2.32
LNi3	25.6	18.6	48.4	7.4
HNi1	12.59	12	73.4	2.21
HNi2	28.22	10.1	56.2	5.48
HNi3	53	0	40.3	12.74

To clarify Mn effect two samples (LNi1 and HNi1) were compared. In former because of low content of alloying elements coarse ferrite grain were visible, however, in later the microstructure was finer with large amount of AF and granular bainite.

HNi1 mostly contained granular bainite that is formed in the same temperature range as AF and nucleation and growth of them is same too. The difference between them is their morphology which bainite first nucleates in austenite grain boundary and grows by unites repetitions, but AF usually

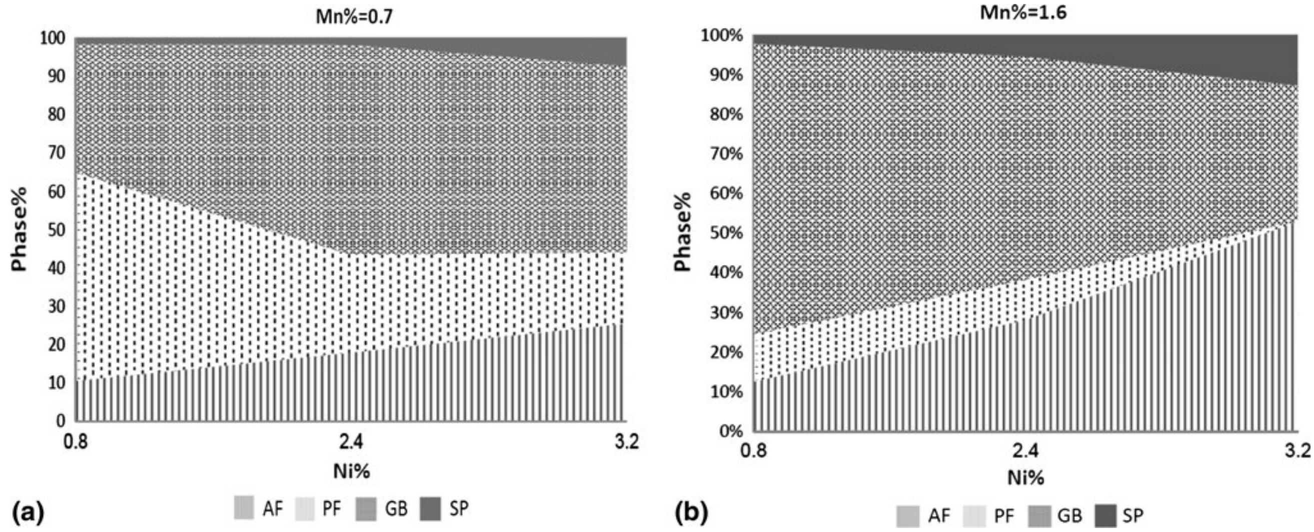

Fig. 7 Different phase amounts in last pass versus Ni% and (a) Mn% = 0.7 and (b) Mn% = 1.6

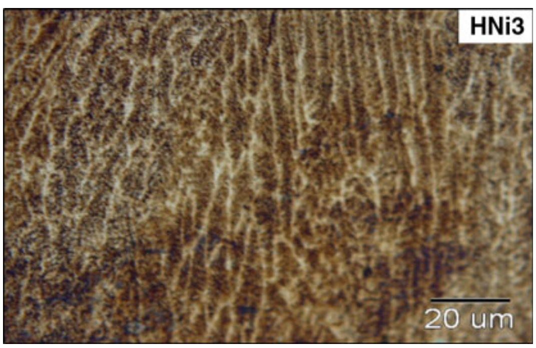

Fig. 8 Microsegregation because of Ni and Mn aggregation

nucleates between the austenite grains on the non-metallic inclusions.

SEM observations of the microstructure of the reheated zone indicated that, the proportion of the AF structure was increased and the polygonal ferrite structure decreased, respectively, and granular bainite and martensite-austenite structure could be found, as the contents of Mn and Ni was increased. Especially, an increase of the Ni content in both levels of Mn, from 2.4 to 3.2% resulted in a significant increase in amount of M-A and a reduce in their size.

3.1.3 Elemental Segregation in Weld Metal. Because of increasing the concentrations of elements such as Mn, Ni, S, P, and Si in liquid during solidification leads to the formation of some dark and light layered nets which resist against the etchant as it is shown in Fig. 8. This structure is deleterious for toughness. The microsegregation is a result of delta ferrite growth from the liquid weld metal. Microsegregation of elements reinforced formation of hard phases in interdendertic zones and increase M-A.

4. Conclusions

With three nickel amount (0.8, 2.4, and 3.2%) and two Mn level (0.7 and 1.6%) addition to the covering of E8018 electrodes, it was possible to produce low alloy electrodes for welding of X80 steel instead of cellulosic electrodes for reduction of hydrogen induced crack risk. The major conclusion of this research can be summarized as follows:

1. A wide range of microstructure, such as various ferrites formed in different proportion of Ni and Mn in columnar zone and reheated zone. At high Mn and Ni concentrations, grain refining did not occurred in reheated zone.
2. The proportion of AF was increased as Ni and Mn contents were increased, and bainite and M-A structure began to arise at the same time.
3. High Mn and Ni contents tend to promote microsegregation of Mn, Ni, and Si in a network or parallel to grain boundaries in reheated zone.

References

1. M.K. Graf and H.G. Hillenbrand, High-Strength Large-Diameter Pipe for Long-Distance High Pressure Gas Pipelines, *IJOPE*, 2004, **14**, p 117–121
2. M.H. Avazkonandeh-Gharavol and M.A. Haddad-Sabzevar, Effect of Copper Content on the Microstructure and Mechanical Properties of Multipass MMA, Low Alloy Steel Weld Metal Deposits, *Mater. Sci. Des.*, 2009, **30**, p 1902–1912
3. A.G. Fox and D.G. Brothers, The Role of Titanium in the Non-Metallic Inclusions with Nucleated Acicular Ferrite in the Submerged Arc Weld Fusion Zone of HY-100 Steel, *Scr. Mater.*, 1995, **13**, p 7661–7666
4. W. Bose-Filho, L.M. Carvalho, and M. Stangwood, Effect of Alloying Elements on the Microstructure and Inclusion Formation in HSLA Multipass Welds, *Mater. Charact.*, 2007, **58**, p 26–39
5. S.C. Hong, S.H. Lim, H.S. Hong, K.J. Lee, D.H. Shin, and K.S. Lee, Effect of Nb on Strain Induced Ferrite Transformation in C-MN steel, *Mater. Sci. Eng. A*, 2003, **355**(1–2), p 241–248
6. S. Bang and Y.W. Kim, Estimation and Prediction of HAZ Softening in Thermo Mechanically Controlled-Rolled and Accelerated-Cooled Steel, *Weld. J.*, 2002, **81**, p 174–179
7. H. Farhat, "Effect of Multiple Wires and Welding Speed on Microstructure and Properties of Submerge Arc Welded X80 Steels," Master Degree Thesis, University of Saskatchewan, 2007, p 20–54
8. S.D. Behole, J. Nemade, B. Collins, and Z.C. Liu, Effect of Nickel and Molybdenum Additions on Weld Metal Toughness in a Submerge Arc Welded HSLA Linepipe Steel, *J. Mater. Process. Technol.*, 2006, **173**, p 92–100

9. A. Goldenberg, A. Sukhikh, and N.P. Mineeva, Effect of Manganese and Nickel on the Strength of Steel Under Rigid Loading Condition, *J. Metalloved. Itermicheskaya Obrab. Metallov.*, 1971, **6**, p 41–43
10. Z. Zhang and R.A. Farrar, Influence of Mn and Ni on the Microstructure and Toughness of C-Mn-Ni Weld Metals, *Weld. J.*, 1997, **76**, p 183–195
11. B.Y. Kang and H.J. Kim, Effect of Mn and Ni on the Variation of the Microstructure and Mechanical Properties of Low-Carbon Weld Metal, *ISIJ Int.*, 2000, **40**(12), p 1237–1245
12. "Specification for Low-Alloy Steel Electrodes for Shielded Metal Arc Welding" ASME 2001, Sec II, Part C-Welding, SFA-5.5, p 99–147